

Channel nuclear pore protein 54 directs sexual differentiation and neuronal wiring required for female reproductive behaviors in *Drosophila*

IRMGARD U. HAUSSMANN^{1,2*}, MOHANAKARTHIK P. NALLASIVAN^{1*}, DANIELA SCOCCHIA¹, ALBERTO CIVETTA³ AND MATTHIAS SOLLER^{1,4}

¹School of Biosciences, College of Life and Environmental Sciences, University of Birmingham, Edgbaston, Birmingham, B15 2TT, United Kingdom

²Department of Life Science, School of Health Sciences, Birmingham City University, Birmingham, B5 3TN, United Kingdom

³Department of Biology, University of Winnipeg, Winnipeg, Canada

Running title: Nup54 directs sexual differentiation

Key Words: Nup54, nuclear pore complex (NPC), sexual differentiation, neuronal wiring, post-mating behaviors, pickpocket (ppk) neurons, doublesex (dsx)

⁴Corresponding author: m.soller@bham.ac.uk

* equal contributing authors

Abstract

The post-mating response induced by male-derived sex-peptide in *Drosophila* females is a well-established model to elucidate how complex innate behaviors are hard-wired into the brain. Here, we found that the channel nuclear pore protein Nup54 is essential for the sex-peptide response as viable mutant alleles do not lay eggs and reduce receptivity upon sex-peptide exposure. Nup54 directs correct wiring of few adult brain neurons that express *pickpocket* and are required for egg laying, but channel Nups also mediate sexual differentiation and male X-chromosome dosage compensation. Consistent with links of Nups to speciation, the Nup54 promoter is a hot spot for rapid evolution and Nup54 is differentially expressed in the brain. These results implicate altered expression of Nup54 to the onset of speciation processes leading to changes in neuronal wiring and sexual differentiation as a response to sexual conflict arising from male-derived SP to direct the female post-mating response.

Introduction

Female reproductive behaviors and physiology change profoundly after mating. Control of pregnancy-associated changes in physiology and behaviors are largely hard-wired into the brain to guarantee reproductive success, yet the gene expression programs that direct neuronal differentiation and wiring at the end of the sex determination pathway are largely unknown.

In most insects, male-derived substances transferred during mating direct female physiology and post-mating behaviors [1-3]. *Drosophila* females display a repertoire of sex specific behaviors after mating including reduced receptivity (readiness to mate) and increased egg laying [4, 5]. The main trigger of these post-mating behaviors is male-derived sex-peptide (SP) [6-9]. SP is a 36 amino acid peptide that is transferred during mating to the female [10]. Besides reducing receptivity and increasing egg laying, SP induces a number of other behavioral and physiological changes including increased egg production, feeding, a change in food choice, sleep, constipation and stimulation of the immune system [11-18]. In addition, SP binds to sperm and acts as a sperm sensor, is required for the release of stored sperm and imposes costs of mating [19-21].

Many of the phenotypic effects of SP on female physiology are known, but central aspects of the neuronal circuitry governing regulation of the main post-mating behaviors like reduced receptivity and increased oviposition are unclear. First insights came from the analysis of *egghead* mutant alleles that are insensitive to SP [22]. In these mutants neuronal connections from the ventral nerve cord to the central brain show defects resulting in an egg retainer phenotype and non-responsiveness to SP in reducing receptivity. This suggests that receptor signaling is disconnected from the motor output programs. Other attempts to map the circuitry mediating the post-mating response used expression of membrane-tethered SP or RNAi knockdown of a receptor for SP, SPR, in distinct neuronal expression

patters [9, 23-27]. These screens identified *pickpocket* (*ppk*), *fruitless* (*fru*) and *dsx* expressing neurons mediating the post-mating switch via expression of membrane-tethered SP in multiple pathways [9].

The ability of males to manipulate post-mating responses of females, for example, by SP in *Drosophila*, can promote sexual conflict and trigger an arms-race between the sexes [28-30]. This arms-race drives rapid evolution and can fuel speciation. Two essential nuclear pore proteins, *Nup96* and *Nup160*, that are part of the outer ring of the pore and interact with each other, trigger inviability in hybrids between species through adaptive divergence in these two proteins [31-34]. The megadalton nuclear pore complex constitutes a bidirectional gateway connecting the nucleus and cytoplasm to control transport of all macromolecules [35], but how nuclear pore proteins can drive speciation is unknown.

Here, we have identified a role for the essential *Nuclear pore protein 54* (*Nup54*) gene, that is part of the nucleo-cytoplasmic transport channel, in constituting the SP response through an allele displaying egg retention and insensitivity to SP with regard to receptivity. *Nup54* is a core protein of the nuclear pore and localizes to the transport channel connecting the nucleus with the cytoplasm. Despite being a constitutive part of the nuclear pore, *Nup54* is differentially expressed in the brain and required early in neuronal development to direct proper wiring of few neurons in the adult brain that express *ppk* and are part of the neuronal circuit directing egg laying. In addition, more general roles for the nuclear pore in regulating sexual differentiation are indicated by RNAi knockdown of channel Nups, which results in differentiation defects of internal and external sexual features in males and females.

Results

Mutant females for *Nup54* alleles display an egg retainer phenotype and are insensitive to sex-peptide for reducing receptivity

To identify novel genes involved in specifying the SP response, we screened females from egg retainer lines that have normal oogenesis, but are unable to lay eggs, for their ability to reduce receptivity [22]. Using this approach, we identified a homozygous viable EMS induced line, *QB62* [36], that did not reduce receptivity upon injection of SP (Figure 1A-D). We mapped this allele by meiotic recombination based on the egg retention phenotype to 2-69.9, corresponding approximatively to chromosome position 50C. Using overlapping deficiencies this allele could then be mapped to chromosome section 49A4 by deficiencies *Df(2R)BSC305* and *Df(2R)Exel16061* (Figure 1A). To further restrict the number of genes in this chromosomal area we generated a smaller deficiency, *Df(2R)9B4*, by FRT mediated recombination between transposons *P{XP}CG8525^{d06853}* and *PBac{RB}DUBAI^{e00699}* (Figure 1A). We then identified a *Mi{ETI}* transposon insert in the *Nup54* gene, *Nup54^{MB03363}*, that was allelic to *QB62* with respect to both egg retention and reduction of receptivity after SP injection (Figure 1B-D). *Nup54* localizes to the transport channel of the megadalton nuclear pore complex that constitutes a bidirectional gateway connecting the nucleus and cytoplasm to control transport of all macromolecules [35]. The *Nup54^{MB03363}* transposon insert leads to a truncation of the *Nup54* ORF and removes the C-terminal alpha helical domain that connects *Nup54* with *Nup58*, but leaves the core part containing the FG repeats composing the inner nuclear channel and the interaction of *Nup54* with *Nup62* via the alpha/beta helical region intact (Figure 1E) [35, 37, 38]. Sequencing of the *Nup54^{QB62}* allele identified a small deletion (CATTAGAGAGGAGGCGTAA) in the promoter region 186 nt upstream of the first transcribed nucleotide suggesting that this allele impacts on the expression of *Nup54* (Figure 1A), possibly only in

a subset of cells, because we did not detect differences by qPCR (Figure S1A). These two alleles represent hypomorphic mutations as channel Nups are essential genes [35].

A genomic rescue using a construct with a deletion of the first intron containing the overlapping gene *CG432041* (*gNup54*) further confirmed that the egg retention and SP insensitivity in receptivity maps to the *Nup54* gene (Figure 1B and C). We then analyzed the expression of Nup54 from *gNup54* via the C-terminal HA tag. In salivary glands, Nup54 localizes to the nuclear membrane. Intriguingly, in both the larval ventral nerve cord and the adult brain, Nup54 expression is dynamic and levels are higher in some cells (Figure S1B-D).

Nup54 is required before neuronal maturation for establishing the post-mating response

Next, we expressed *Nup54* from a *UAS* construct in a *Nup54^{MB03363}/Df(2R)9B4* background to identify its temporal and spatial requirement for rescuing the egg retainer and SP insensitivity phenotype in receptivity. Global expression with *tubGAL4* in *Nup54^{MB03363}/Df(2R)9B4* completely rescued these phenotypes after injection of SP. We then expressed *UASNup54* in all differentiated neurons with *elavGAL4^{C155}* or in subsets using *ppkGAL4*, *fruGAL4* and *dsxGAL4* to test whether they can rescue the post-mating response in *Nup54^{MB03363}/Df(2R)9B4* after SP injection (Figure S2A and B). These experiments revealed that *fruGAL4* and *dsxGAL4*, which express earlier than *elav*, can rescue the SP insensitivity and suppress remating, but only *dsxGAL4* can marginally rescue egg laying (Figure S2A and B).

Taken together these data indicate that Nup54 is required early in development before neurons are fully differentiated to specify the neuronal circuits required for the post-mating response.

***Nup54^{QB62}* displays defects in neuronal wiring of *pickpocket* expressing neurons**

Expression of membrane-bound SP can induce the post-mating response in *ppk* expressing neurons [23-26]. To examine whether Nup54 function is required for neuronal wiring relevant for the post-mating response, we visualized neuronal projections of *ppk* neurons in wild type and *Nup54^{QB62}/Df(2R)9B4* mutant females by expression of CD8::GFP from *UAS* under the control of *ppkGAL4*. In the larval brain of control females *ppk* sensory neuronal projections display a regular pattern of connectives and commissures, while in *Nup54^{QB62}/Df(2R)9B4* mutants many connectives and commissures are disrupted (Figure 2A-F). In the adult brain, projections in the central brain were dramatically reduced in *Nup54^{QB62}/Df(2R)9B4* females compared to control females (Figure 2G and H). So far it has been shown that *ppk* expresses in sensory neurons projecting to the brain [23-26]. A closer examination of *ppk* expression in the adult female brain, however, revealed four paired neurons consistently expressing a nuclear histon2B::YFP marker expressed from *UAS* with *ppkGAL4*. Strikingly, these neurons lacked projections in *Nup54^{QB62}/Df(2R)9B4* females (Figure 2G-I).

***ppk* neurons in the brain are part of the circuit required for egg laying**

To test whether *ppk* expressing neurons in the brain are involved in the post-mating response we used an intersectional gene expression approach based on brain-specific expression of *orthodentical* (*otd*) to specifically inhibit neuronal transmission in brain *ppk* neurons by expression of tetanus-toxin (TNT) [39]. To achieve restricted expression of TNT in *ppk* brain neurons, we crossed *otd-flipase* (*otd::flp*) flies with *ppkGAL4*, *UAS FRTGFPstopFRT TNT* flies and analysed the female progeny for PMRs (Figure 3A).

These experiments revealed that females with inhibited *ppk* neurons in the brain displayed a compromised response to SP as they did not fully reduce receptivity and did not lay the eggs stored in the ovaries after injection of SP (Figure 3B-D). In contrast, inhibition of all *ppk* neurons partially reduced

receptivity in SP injected females. In addition, these females display increased egg laying as virgins, but SP does not further enhance egg laying (Figure 3B-D). Control females of *UAS TNT* without a *GAL4* driver showed a normal response to SP (data not shown).

Taken together, these results demonstrate an essential role for *ppk* neurons in the brain in inducing egg laying, and a partial requirement for reducing receptivity in response to SP.

Specification of neuronal circuits for receptivity and egg laying are separable

To further test the role of *Nup54* in the post-mating response we used *UASRNAi* knock-down of *Nup54* in either all neurons using *elavGAL4^{C155}*, or in subsets of neurons using *ppkGAL4*, *fruGAL4* and *dsxGAL4*. RNAi knock-down of *Nup54* with *elavGAL4^{C155}*, *ppkGAL4* and *fruGAL4* did not affect receptivity, or egg laying after SP injection further demonstrating that *Nup54* is required early in neuronal development (Figure S3A and B). In contrast, RNAi knock-down of *Nup54* with *dsxGAL4*, oviposition was not induced upon SP injection while receptivity was reduced normally (Figure S3A and B).

In summary, the combined results from experiments in Figure S2A and B, and Figure S3A and B indicate that *Nup54* is required early in neuronal development and that the neuronal circuits for egg laying and receptivity are specified by distinct neuronal populations.

Channel Nups have a role in sex determination and dosage compensation

When knocking down *Nup54* with RNAi using *dsxGAL4*, we noticed that females laid eggs that did not develop. In addition, male survival was low (20%, n=107, *P*{*TRIP.HMC04733*}) or males were completely absent (n=107, *P*{*GDI4041*}v42153; *P*{*GDI4041*}v42154), indicating that *Nup54* has additional roles in dosage compensation [40, 41]. Therefore, we hypothesized that the other two channel

Nups, Nup58 and Nup62, that form a complex with Nup54, also have roles in specifying the post-mating response and/or in sexual differentiation and dosage compensation. RNAi knockdown of *Nup58* (*P{TRIP.HMC05104}*) with *dsxGAL4* resulted in lethality with only few very weak female escapers. These females, however, were sterile due to the lack of ovaries and deformed genitals. Similar results were obtained by RNAi knock-down of *Nup62* with *dsxGAL4* resulting in male lethality (9%, n=81 and 2%, n=45 escapers with *P{TRIP.GLV21060}* and *P{TRIP.HMC03668}* Since) and females without ovaries (100%, n=74 and 43%, n=35 with *P{TRIP.GLV21060}* and *P{TRIP.HMC03668}*). In addition, these females also had deformed genitals and males displayed underdeveloped sex combs indicating a role for channel Nups in sexual differentiation (Figure S3C-F). Consistent with a regulatory role in development, the channel Nups display dynamic expression during development and in different tissues (Figure S4A-F).

The role of insertion/deletion (indels) during the evolution of Nup54 function

Adaptation to new situations drives the evolution of hybrid incompatibility genes *Nup96* and *Nup160* [31-34]. Here, we used the combined analysis of polymorphism within *D. melanogaster* and divergence between *D. melanogaster* and *D. simulans* within the coding region of *Nup54* to test for deviations from expectations under the neutral model of molecular evolution. We found no deviation from the null neutral model hypothesis, as the ratio of nonsynonymous to synonymous polymorphisms did not significantly differed from the ratio of nonsynonymous to synonymous fixed differences between species (MK test: $\chi^2=0.09$; $P=0.923$). The test was also non-significant when we partition the analysis by exons. Also, the upstream noncoding region did not significantly depart from neutrality (Fisher's exact test $P=0.135$), but there was a trend towards an excess of upstream noncoding relative to silent (synonymous

and intron) substitutions between species ($d_{NC}/d_S=3.1$) relative to polymorphisms within *D. melanogaster* ($P_{NC}/P_S=2.0$) (neutrality index: $NI = 0.65$).

Indels are a common form of genetic variation, being able to affect gene function and their pattern of evolution being subjected to selective forces [42-44]. We noticed that a stretch of amino acids of increasing length in more distantly related species is inserted in the FG repeat region (Figure S5A). We therefore hypothesized that this indel could alter the function of Nup54 in specifying the post-mating response. To test this hypothesis, we replaced the FG-repeat region from *D. melanogaster* with the region from *D. elegans* in the genomic rescue construct *gNup54ele* and tested its capacity to rescue viability of *Df(2R)9B4* and the post-mating response defects. Both the *D. melanogaster gNup54* and the chimeric *D. elegans gNup54ele* rescued viability of *Df(2R)9B4* to 91% (n=242) and 95% (n=381) without sex-bias, respectively. After injection of SP, females rescued with the *gNup54* or the *gNup54ele* construct showed normal post-mating responses in receptivity and oviposition arguing that this indel is not the source for an altered post-mating response (Figure S5B and C).

In the *Nup54* promoter region rapid evolution is identifiable by the presence of four hotspots for substitutions between species, all within 1 kb upstream of the *Nup54* transcription start site (Figure 4A and B). Interestingly, one substitutional hotspot (-359 to -295) includes an indel that overlaps with the location of the characterized *Nup54^{QB62}* regulatory allele (Figure 4B). The deletion in the *Nup54^{QB62}* allele in fact is to a large extent a wild type condition in sister species (Figure 4A). While it is unclear whether this change has been driven by selection, it has clearly evolved in the context of the post-mating response to SP.

Discussion

Here we show that Nup54 which is part of the central transport channel of the nuclear pore exerts a role in specifying the neuronal circuits involved in mediating the SP induced post-mating switch. Viable alleles of these genes display an egg retainer phenotype and are insensitive to SP with regard to reducing receptivity. Nup54 is required for wiring of *ppk* expressing neurons in the brain that constitute part of the circuitry required for egg laying. The role of Nup54 and the other two channel Nups, Nup58 and Nup62, in sexual differentiation, however, seems to be more fundamental as reducing their expression levels impacts on general sexual differentiation of external and internal sexual features, such as female genitals and ovaries, but also on dosage compensation in males.

Roles for Nups in development

A key role for Nups in sexual differentiation seems rather unexpected as the function of channel Nups in directing constitutive export of mRNAs and proteins from the nucleus to the cytoplasm has been viewed as static for a long time. However, a number of recent studies have brought about developmental and neuronal roles for the nuclear pore and nucleocytoplasmic transport reflected in a number human diseases including neurodegeneration associated with specific Nups [45-47]. A central aspect of these more profound roles for Nups lay in their varying expression levels between different cell types, tissues and in development. Nup210's key role in muscle and neuronal differentiation are associated with tissue-specific expression [48]. Likewise, high expression levels of Nup153 are critical for maintenance of ESC pluripotency as reducing levels results in neuronal differentiation [49]. Also, channel Nup62 shows increased expression in various epithelia and is required for proliferation [50]. In *Drosophila*, channel Nups 54, 58 and 62 show increased expression in the larval brain and adult gonads [51]. Our findings that channel Nups have a role in sexual differentiation add to this view that the nuclear pore has key roles in differentiation and likely also neuronal function.

Specification of neuronal circuits for receptivity and egg laying are separable

It has previously been argued that the neurons co-expressing *fru*, *dsx* and *ppk* in the genital tract sense SP and direct the SP induced post-mating [24-26]. However, our data from expressing a *Nup54* rescue construct and from RNAi knockdown in various cell types suggests a more complex picture including separation of the paths leading to reduced receptivity and increased egg laying. Here, expression of *Nup54* in *fru* and *dsx* neurons, but not *ppk* neurons rescues receptivity while egg laying is not rescued in all three expression patterns. Also, RNAi of *Nup54* in *dsx* neurons leads to inhibition of egg laying, but receptivity is reduced normally. RNAi in *fru* and *ppk* neurons has no effect on SP induced changes in receptivity and egg laying. Although the latter effect could be explained by different expression levels of *fru*, *dsx* and *ppk* GAL4 lines, this is not observed and they express strongly. Consistent with a requirement for *Nup54* early in development, *dsx* is expressed earlier than *fru* and *ppk*. Differential effects on receptivity, but not egg laying by *dsx* driven rescue or knock-down by *Nup54*, however, more likely indicates that receptivity and egg laying are governed by different neuronal circuits. These results are supported by previous observations, that G(o) is not required in *fru*, but needed in *dsx* and *ppk* neurons to reduce receptivity [9]. Likewise, membrane-tethered SP can only induce oviposition in the absence of SPR in *dsx*, but not *fru* and *ppk* neurons [9].

Roles of Nups in speciation

New species can arise through selection of new features enhancing display of sexual attributes and altered courtship behavior. A driving force to speciation can be sexual conflict imposed by male-directed post-mating responses by females [28-30]. In *Drosophila melanogaster*, females respond to male-derived SP by reducing receptivity and increasing egg laying, but need to adapt their physiological status

to environmental conditions. Thus, the possibility to limit the male influence imposed by SP is in the female interest of optimizing reproductive success when resources to produce eggs are scarce. In this context, Nup54 regulation could impact on egg laying in dedicated circuits such as brain *ppk* neurons. Consistent with this interpretation, the Nup54 promoter region has undergone a dramatic change compared to closely related species, while no adaptive changes were detected in the protein coding part. Likewise, exchanging the FG repeat of Nup54 mediating nucleo-cytoplasmic transport, which shows most variability between *D. melanogaster*, *D. elegans* and other closely related species had little impact on the post-mating response. Since Nup54 is required in all cells, varying its concentration could have profound effects on general expression of genes and select for a specific compensatory genetic element from the mating partner to prevent deleterious effects on the fitness of the progeny[31-34]. Such interpretation is well in line with roles of essential Nup96 and Nup160 in speciation as they have been identified in causing hybrid sterility or lethality. Intriguingly however, Nup96 and Nup160 are part of the larger NUP107 subcomplex and four out of eight proteins from this complex are under adaptive selection in *D. simulans* [32]. The driving forces behind the role of Nups in speciation and the molecular mechanism leading to speciation, however, need to be further explored.

Here we have identified a few *ppk* expressing neurons in the brain as a cellular focus preventing female escape from male manipulation. Changes in neuronal wiring likely directed in response to sexual conflict arising from male-derived SP to direct the female post-mating response marks an early event in the splitting of species and links differentiation of key neurons involved in female control of reproduction to fitness as a result of sexual conflict. Our results indicate a central role for the nuclear pore in implementing alterations of gene expression impacting on neuronal wiring at the onset of speciation processes.

Materials and Methods

Flies were kept on standard cornmeal-agar food (1% industrial-grade agar, 2.1% dried yeast, 8.6% dextrose, 9.7% cornmeal and 0.25% Nipagin, all in (w/v)) in a 12 h light : 12 h dark cycle. Sexually mature 3–5 day-old virgin females were injected and examined for their post-mating behaviors as described previously [12, 22]. For injections, virgin female flies were cooled to 4° C and 3 pmol SP in 50 nl Ringer's solution was injected. Ovaries were analyzed as previously described [12]. ANOVA followed by planned pairwise comparisons with Fisher's protected least significant difference was done for statistical analysis using STATVIEW or Graphpad prism.

The *UAS* construct with a N-terminally HA-tagged Nup54 was generated in a three way ligation with fragments of *Nup54* amplified from cDNA by RT-PCR that were cloned into a modified *pUC*, *pUC 3GLA UAS HA*, with NheI and Acc65I with a blunt site in between. The 5' part was amplified using primers 8831F1 (CATCGCTAGCGCCTGCAGGATCGTTCTTCGGATCCAACACGTCGCTGG) and 8831R1 (CTGAGAGTTCTCTGCAGAAGTTAAGAGCCAC), and the 3' part with primers 8831F2 (CTGTCAAGCCACACCAGCAACAAGTGATTC) and 8831R2 (GACAGGTACCTATCACGATTGTCGCAGCTCGGGCAGTC) by PCR with Pwo (Roche) and sequenced. The genomic rescue construct was generated in a three way ligation by cloning the promoter fragment amplified from genomic DNA with primers 8831F1g (GTGGAATTCCGGAGGCCACTAGAACATATACTTGTC) and 8831R1g (GGCGTGCTTGTTGCTCCCAGCGACGTGTTG) and the cDNA part amplified from the *UAS* construct with primers 8831F3 (GGCCAAAACAACCGGTGGCCTCTTCGGATC) and 8831R3 (GGCGTGCTTGTTGCTCCCAGCGACGTGTTGTAGCTCGAGGATTGTCGCAGCTCGGGCAGTC) using EcoRI and XhoI sites into a modified *pUC*, *pUC 3GLA* that adds a C-terminal HA tag and sequenced [52]. The *D. elegans* rescue construct was generated in a three way ligation by replacing the

part between NgoMIV and MfeI with the corresponding part amplified from *D. elegans* cDNA by RT-PCR with primers 8831Fele (CCAAAACAACcGGaGGCCTCTTCGGAAC) and 8831R1ele (CGTGGATCCGAAGGCTCCGCCCCCAAAGCCAGTG), and a BamHI/MfeI fragment obtained from the UAS construct. Transgenic flies were generated by phiC31-mediated transformation using landing site 76A (*PBac{y+ -attP-3B}VK00002*), where the GFP marker had been removed by Cre/Lox mediated recombination. *Df(2R)9B4* was generated by FLP/FRT-mediated recombination between two transposon insertion lines, *P{XP}CG8525^{d06853}* and *PBac{RB}DUBAI^{e00699}* as described [53, 54]. The *tubGal4* line was a third chromosomal insert (Bloomington #5138), *UAS FRTGFPstopFRT TNT* and the other lines have been previously described [9, 55, 56]. Antibody stainings were done as previously described [57, 58].

Genomic DNA was extracted from *Nup54^{QB62}* as described [59]. The promoter fragment was amplified with primers 8831pF1 (GGATCTGGTGAGCAGAGGTTGCGATG) and 8831pR1 (GCCGCACAGTTTGGGTTGCCTTTC) and sequenced. Reverse transcription quantitative polymerase chain reaction (RT-qPCR) was done by extracting total RNA using Tri-reagent (SIGMA) and RT was done with Superscript II (Invitrogen) according to the manufacturers instructions using an oligo dT primer. For qPCR 1.5 µl cDNA with the SensiFAST SYBR No-Rox kit (Bioline) was used with primers Nup54qF1 (CTGCCACAGCGAAGATACT) and Nup54qR1 (CAGCATGTTCTGTAGCTTGGTGC), and ewg4F1 and ewg5R1 [60]. Amplification was done in a Applied Biosystems ABI Prism 7000 with 3 min initial denaturation at 95° C followed by 40 cycles with 15 sec denaturation at 95°C and 60 sec extension at 60° C. Quantification was done according to the Δ CT method [61].

Structural analysis was done by PyMol. The *Nup54* ORF and extended gene sequences were retrieved from FlyBase (flybase.org) and aligned using muscle within MEGA (reference). *D. melanogaster* polymorphism data was retrieved from the Drosophila Genetic Reference Panel

(<http://dgrp2.gnets.ncsu.edu/>) and used along with interspecies divergence data (*D. melanogaster* – *D. simulans*) to conduct McDonald Kreitman's tests of selection for the ORF and extended gene region. Tests were conducted by comparing nonsynonymous to synonymous substitutions and polymorphisms (ORF) as well as noncoding upstream to silent (within gene synonymous and intron) substitutions and polymorphism [62-64].

We also tested for evidence of nonrandom accumulation of substitutions along the *Nup54* extended gene region. The method tests for significant deviations from a uniform distribution of substitutions using an empirical cumulative distribution function. The function (G) detects monotonic increases in substitutions (n) measured as the difference between the relative occurrence of a nucleotide change and its relative position in the alignment [65, 66]. Whether differences between the values of the G function (ΔG) between substitutional events deviates from a random accumulation of changes are tested using Monte Carlo simulations to produce 100,000 samples of n events by sampling sites without replacement along the alignment [65, 66].

Acknowledgments

We thank T. Schüpbach, B. Dickson, S. Goodwin, C. Rezaval, D. Anderson, the Bloomington stock center, the Vienna Drosophila RNAi Center and the Arizona species stock center for fly lines and the University of Cambridge Department of Genetics Fly Facility for injections, N. Arora for help with behavioral assays and T. Dix for help with PyMol, C. Rezaval and J.C. Billeter for comments on the manuscript. We are indebted to Eric Kubli for his support when this study was initiated. This work was supported by the Biotechnology and Biological Science Research Council to MS and the Natural Sciences and Engineering Research Council of Canada to AC.

Authors' contribution

MS conceived and directed the project. IUH, DS and MS performed molecular biology experiments, IUH, MN, DS and MS performed genetic experiments, and AC performed sequence analysis. All authors analyzed data. MS wrote the manuscript with support from IUH and AC. All authors read and approved the final manuscript.

Competing interests

The authors declare that they have no competing interests.

References

1. Gillott C. Male accessory gland secretions: Modulators of Female Reproductive Physiology and Behavior. *Annu Rev Entomol.* 2003;48(1):163-84.
2. Griffith LC. Neuroscience: love hangover. *Nature.* 2008;451(7174):24-5. Epub 2008/01/04. doi: 451024a [pii]
10.1038/451024a. PubMed PMID: 18172487; PubMed Central PMCID: PMC2742166.
3. Avila FW, Sirot LK, LaFlamme BA, Rubinstein CD, Wolfner MF. Insect seminal fluid proteins: identification and function. *Annu Rev Entomol.* 2011;56:21-40. Epub 2010/09/28. doi: 10.1146/annurev-ento-120709-144823. PubMed PMID: 20868282.
4. Kubli E. Sex-peptides: seminal peptides of the *Drosophila* male. *Cell Mol Life Sci.* 2003;60(8):1689-704.
5. Kubli E. Sexual behaviour: a receptor for sex control in *Drosophila* females. *Curr Biol.* 2008;18(5):R210-2. Epub 2008/03/13. doi: S0960-9822(07)02444-X [pii]

10.1016/j.cub.2007.12.047. PubMed PMID: 18334196.

6. Liu H, Kubli E. Sex-peptide is the molecular basis of the sperm effect in *Drosophila melanogaster*. *Proc Natl Acad Sci U S A*. 2003;100(17):9929-33. PubMed PMID: 12897240.
7. Aigaki T, Fleischmann I, Chen PS, Kubli E. Ectopic expression of sex peptide alters reproductive behavior of female *D. melanogaster*. *Neuron*. 1991;7(4):557-63.
8. Chapman T, Bangham J, Vinti G, Seifried B, Lung O, Wolfner MF, et al. From the Cover: The sex peptide of *Drosophila melanogaster*: Female post-mating responses analyzed by using RNA interference. *PNAS*. 2003;100(17):9923-8.
9. Haussmann IU, Hemani Y, Wijesekera T, Dauwalder B, Soller M. Multiple pathways mediate the sex-peptide-regulated switch in female *Drosophila* reproductive behaviours. *Proc Biol Sci*. 2013;280(1771):20131938. Epub 2013/10/04. doi: rspb.2013.1938 [pii]
10.1098/rspb.2013.1938. PubMed PMID: 24089336; PubMed Central PMCID: PMC3790487.
10. Chen PS, Stumm-Zollinger E, Aigaki T, Balmer J, Bienz M, Bohlen P. A male accessory gland peptide that regulates reproductive behavior of female *D. melanogaster*. *Cell*. 1988;54(3):291-8.
11. Soller M, Bownes M, Kubli E. Mating and Sex Peptide Stimulate the Accumulation Of Yolk In Oocytes Of *Drosophila Melanogaster*. *European Journal of Biochemistry*. 1997;243(3):732-8.
12. Soller M, Bownes M, Kubli E. Control of oocyte maturation in sexually mature *Drosophila* females. *Dev Biol*. 1999;208(2):337-51.
13. Carvalho GB, Kapahi P, Anderson DJ, Benzer S. Allocrine modulation of feeding behavior by the Sex Peptide of *Drosophila*. *Curr Biol*. 2006;16(7):692-6. PubMed PMID: 16581515.
14. Isaac RE, Li C, Leedale AE, Shirras AD. *Drosophila* male sex peptide inhibits siesta sleep and promotes locomotor activity in the post-mated female. *Proc Biol Sci*. 2010;277(1678):65-70. Epub 2009/10/02. doi: rspb.2009.1236 [pii]

10.1098/rspb.2009.1236. PubMed PMID: 19793753; PubMed Central PMCID: PMC2842620.

15. Ribeiro C, Dickson BJ. Sex peptide receptor and neuronal TOR/S6K signaling modulate nutrient balancing in *Drosophila*. *Curr Biol*. 2010;20(11):1000-5. Epub 2010/05/18. doi: S0960-9822(10)00387-8 [pii]

10.1016/j.cub.2010.03.061. PubMed PMID: 20471268.

16. Peng J, Zipperlen P, Kubli E. *Drosophila* sex-peptide stimulates female innate immune system after mating via the Toll and Imd pathways. *Curr Biol*. 2005;15(18):1690-4. PubMed PMID: 16169493.

17. Domanitskaya EV, Liu H, Chen S, Kubli E. The hydroxyproline motif of male sex peptide elicits the innate immune response in *Drosophila* females. *FEBS J*. 2007;274(21):5659-68. Epub 2007/10/10. doi: EJB6088 [pii]

10.1111/j.1742-4658.2007.06088.x. PubMed PMID: 17922838.

18. Cognigni P, Bailey AP, Miguel-Aliaga I. Enteric neurons and systemic signals couple nutritional and reproductive status with intestinal homeostasis. *Cell Metab*. 2011;13(1):92-104. Epub 2011/01/05. doi: 10.1016/j.cmet.2010.12.010. PubMed PMID: 21195352; PubMed Central PMCID: PMC3038267.

19. Peng J, Chen S, Busser S, Liu H, Honegger T, Kubli E. Gradual Release of Sperm Bound Sex-Peptide Controls Female Postmating Behavior in *Drosophila*. *Current Biology*. 2005;15(3):207-13.

20. Avila FW, Ravi Ram K, Bloch Qazi MC, Wolfner MF. Sex peptide is required for the efficient release of stored sperm in mated *Drosophila* females. *Genetics*. 2010;186(2):595-600. Epub 2010/08/04. doi: genetics.110.119735 [pii]

10.1534/genetics.110.119735. PubMed PMID: 20679516; PubMed Central PMCID: PMC2954482.

21. Wigby S, Chapman T. Sex peptide causes mating costs in female *Drosophila melanogaster*. *Curr Biol*. 2005;15(4):316-21. PubMed PMID: 15723791.
22. Soller M, Haussmann IU, Hollmann M, Choffat Y, White K, Kubli E, et al. Sex-peptide-regulated female sexual behavior requires a subset of ascending ventral nerve cord neurons. *Curr Biol*. 2006;16(18):1771-82. PubMed PMID: 16979554.
23. Nakayama S, Kaiser K, Aigaki T. Ectopic expression of sex-peptide in a variety of tissues in *Drosophila* females using the P[GAL4] enhancer-trap system. *Mol Gen Genet*. 1997;254(4):449-55. Epub 1997/04/28. PubMed PMID: 9180699.
24. Hasemeyer M, Yapici N, Heberlein U, Dickson BJ. Sensory neurons in the *Drosophila* genital tract regulate female reproductive behavior. *Neuron*. 2009;61(4):511-8. Epub 2009/03/03. doi: S0896-6273(09)00076-2 [pii] 10.1016/j.neuron.2009.01.009. PubMed PMID: 19249272.
25. Yang CH, Rumpf S, Xiang Y, Gordon MD, Song W, Jan LY, et al. Control of the postmating behavioral switch in *Drosophila* females by internal sensory neurons. *Neuron*. 2009;61(4):519-26. Epub 2009/03/03. doi: S0896-6273(08)01093-3 [pii] 10.1016/j.neuron.2008.12.021. PubMed PMID: 19249273; PubMed Central PMCID: PMC2748846.
26. Rezaval C, Pavlou HJ, Dornan AJ, Chan YB, Kravitz EA, Goodwin SF. Neural circuitry underlying *Drosophila* female postmating behavioral responses. *Curr Biol*. 2012;22(13):1155-65. Epub 2012/06/05. doi: S0960-9822(12)00518-0 [pii] 10.1016/j.cub.2012.04.062. PubMed PMID: 22658598; PubMed Central PMCID: PMC3396843.
27. Yapici N, Kim YJ, Ribeiro C, Dickson BJ. A receptor that mediates the post-mating switch in *Drosophila* reproductive behaviour. *Nature*. 2008;451(7174):33-7. PubMed PMID: 18066048.

28. Sirot LK, Wong A, Chapman T, Wolfner MF. Sexual conflict and seminal fluid proteins: a dynamic landscape of sexual interactions. *Cold Spring Harb Perspect Biol.* 2014;7(2):a017533. Epub 2014/12/17. doi: 10.1101/cshperspect.a017533. PubMed PMID: 25502515; PubMed Central PMCID: PMC4315932.
29. Chapman T. Sexual Conflict: Mechanisms and Emerging Themes in Resistance Biology. *Am Nat.* 2018;192(2):217-29. Epub 2018/07/18. doi: 10.1086/698169. PubMed PMID: 30016167.
30. Hollis B, Koppik M, Wensing KU, Ruhmann H, Genzoni E, Erkosar B, et al. Sexual conflict drives male manipulation of female postmating responses in *Drosophila melanogaster*. *Proc Natl Acad Sci U S A.* 2019;116(17):8437-44. Epub 2019/04/10. doi: 10.1073/pnas.1821386116. PubMed PMID: 30962372; PubMed Central PMCID: PMC6486729.
31. Presgraves DC, Balagopalan L, Abmayr SM, Orr HA. Adaptive evolution drives divergence of a hybrid inviability gene between two species of *Drosophila*. *Nature.* 2003;423(6941):715-9. Epub 2003/06/13. doi: 10.1038/nature01679. PubMed PMID: 12802326.
32. Presgraves DC, Stephan W. Pervasive adaptive evolution among interactors of the *Drosophila* hybrid inviability gene, Nup96. *Mol Biol Evol.* 2007;24(1):306-14. Epub 2006/10/24. doi: 10.1093/molbev/msl157. PubMed PMID: 17056646.
33. Tang S, Presgraves DC. Evolution of the *Drosophila* nuclear pore complex results in multiple hybrid incompatibilities. *Science.* 2009;323(5915):779-82. Epub 2009/02/07. doi: 10.1126/science.1169123. PubMed PMID: 19197064; PubMed Central PMCID: PMC2826207.
34. Presgraves DC. The molecular evolutionary basis of species formation. *Nat Rev Genet.* 2010;11(3):175-80. Epub 2010/01/07. doi: 10.1038/nrg2718. PubMed PMID: 20051985.

35. Lin DH, Hoelz A. The Structure of the Nuclear Pore Complex (An Update). *Annu Rev Biochem.* 2019;88:18.1-.59. Epub 2019/03/19. doi: 10.1146/annurev-biochem-062917-011901. PubMed PMID: 30883195.
36. Schupbach T, Wieschaus E. Female sterile mutations on the second chromosome of *Drosophila melanogaster*. II. Mutations blocking oogenesis or altering egg morphology. *Genetics.* 1991;129(4):1119-36. Epub 1991/12/01. PubMed PMID: 1783295; PubMed Central PMCID: PMC1204776.
37. Solmaz SR, Chauhan R, Blobel G, Melcak I. Molecular architecture of the transport channel of the nuclear pore complex. *Cell.* 2011;147(3):590-602. Epub 2011/11/01. doi: 10.1016/j.cell.2011.09.034. PubMed PMID: 22036567; PubMed Central PMCID: PMC3431207.
38. Chug H, Trakhanov S, Hulsman BB, Pleiner T, Gorlich D. Crystal structure of the metazoan Nup62*Nup58*Nup54 nucleoporin complex. *Science.* 2015;350(6256):106-10. Epub 2015/08/22. doi: 10.1126/science.aac7420. PubMed PMID: 26292704.
39. Asahina K, Watanabe K, Duistermars BJ, Hoopfer E, Gonzalez CR, Eyjolfsson EA, et al. Tachykinin-expressing neurons control male-specific aggressive arousal in *Drosophila*. *Cell.* 2014;156(1-2):221-35. Epub 2014/01/21. doi: 10.1016/j.cell.2013.11.045. PubMed PMID: 24439378; PubMed Central PMCID: PMC3978814.
40. Haussmann IU, Bodi Z, Sanchez-Moran E, Mongan NP, Archer N, Fray RG, et al. m6A potentiates Sxl alternative pre-mRNA splicing for robust *Drosophila* sex determination. *Nature.* 2016;540(7632):301-4. Epub 2016/12/06. doi: nature20577 [pii] 10.1038/nature20577. PubMed PMID: 27919081.
41. Schutt C, Nothiger R. Structure, function and evolution of sex-determining systems in Dipteran insects. *Development.* 2000;127(4):667-77. Epub 2000/01/29. PubMed PMID: 10648226.

42. Barton HJ, Zeng K. The Impact of Natural Selection on Short Insertion and Deletion Variation in the Great Tit Genome. *Genome Biol Evol.* 2019;11(6):1514-24. Epub 2019/03/30. doi: 10.1093/gbe/evz068. PubMed PMID: 30924871; PubMed Central PMCID: PMC6543879.
43. Chintalapati M, Dannemann M, Prufer K. Using the Neandertal genome to study the evolution of small insertions and deletions in modern humans. *BMC Evol Biol.* 2017;17(1):179. Epub 2017/08/06. doi: 10.1186/s12862-017-1018-8. PubMed PMID: 28778150; PubMed Central PMCID: PMC5543596.
44. Kvikstad EM, Duret L. Strong heterogeneity in mutation rate causes misleading hallmarks of natural selection on indel mutations in the human genome. *Mol Biol Evol.* 2014;31(1):23-36. Epub 2013/10/12. doi: 10.1093/molbev/mst185. PubMed PMID: 24113537; PubMed Central PMCID: PMC3879449.
45. Raices M, D'Angelo MA. Nuclear pore complex composition: a new regulator of tissue-specific and developmental functions. *Nat Rev Mol Cell Biol.* 2012;13(11):687-99. Epub 2012/10/24. doi: 10.1038/nrm3461. PubMed PMID: 23090414.
46. Kim HJ, Taylor JP. Lost in Transportation: Nucleocytoplasmic Transport Defects in ALS and Other Neurodegenerative Diseases. *Neuron.* 2017;96(2):285-97. Epub 2017/10/13. doi: 10.1016/j.neuron.2017.07.029. PubMed PMID: 29024655; PubMed Central PMCID: PMC5678982.
47. Solomon DA, Stepto A, Au WH, Adachi Y, Diaper DC, Hall R, et al. A feedback loop between dipeptide-repeat protein, TDP-43 and karyopherin-alpha mediates C9orf72-related neurodegeneration. *Brain.* 2018;141(10):2908-24. Epub 2018/09/22. doi: 10.1093/brain/awy241. PubMed PMID: 30239641; PubMed Central PMCID: PMC6158706.

48. D'Angelo MA, Gomez-Cavazos JS, Mei A, Lackner DH, Hetzer MW. A change in nuclear pore complex composition regulates cell differentiation. *Dev Cell*. 2012;22(2):446-58. Epub 2012/01/24. doi: 10.1016/j.devcel.2011.11.021. PubMed PMID: 22264802; PubMed Central PMCID: PMCPMC3288503.
49. Jacinto FV, Benner C, Hetzer MW. The nucleoporin Nup153 regulates embryonic stem cell pluripotency through gene silencing. *Genes Dev*. 2015;29(12):1224-38. Epub 2015/06/18. doi: 10.1101/gad.260919.115. PubMed PMID: 26080816; PubMed Central PMCID: PMCPMC4495395.
50. Hazawa M, Lin DC, Kobayashi A, Jiang YY, Xu L, Dewi FRP, et al. ROCK-dependent phosphorylation of NUP62 regulates p63 nuclear transport and squamous cell carcinoma proliferation. *EMBO Rep*. 2018;19(1):73-88. Epub 2017/12/09. doi: 10.15252/embr.201744523. PubMed PMID: 29217659; PubMed Central PMCID: PMCPMC5757218.
51. Brown JB, Boley N, Eisman R, May GE, Stoiber MH, Duff MO, et al. Diversity and dynamics of the *Drosophila* transcriptome. *Nature*. 2014;512(7515):393-9. Epub 2014/03/29. doi: 10.1038/nature12962. PubMed PMID: 24670639; PubMed Central PMCID: PMCPMC4152413.
52. Haussmann IU, Ustaoglu P, Brauer U, Hemani Y, Dix TC, Solter M. Plasmid-based gap-repair recombineered transgenes reveal a central role for introns in mutually exclusive alternative splicing in Down Syndrome Cell Adhesion Molecule exon 4. *Nucleic Acids Res*. 2019;47:1389-403. Epub 2018/12/13. doi: 10.1093/nar/gky1254. PubMed PMID: 30541104; PubMed Central PMCID: PMCPMC6379703.
53. Parks AL, Cook KR, Belvin M, Dompe NA, Fawcett R, Huppert K, et al. Systematic generation of high-resolution deletion coverage of the *Drosophila melanogaster* genome. *Nat Genet*. 2004;36(3):288-92. Epub 2004/02/26. doi: 10.1038/ng1312
ng1312 [pii]. PubMed PMID: 14981519.

54. Thibault ST, Singer MA, Miyazaki WY, Milash B, Dompe NA, Singh CM, et al. A complementary transposon tool kit for *Drosophila melanogaster* using P and piggyBac. *Nat Genet.* 2004;36(3):283-7. Epub 2004/02/26. doi: 10.1038/ng1314
ng1314 [pii]. PubMed PMID: 14981521.
55. Stockinger P, Kvitsiani D, Rotkopf S, Tirian L, Dickson BJ. Neural circuitry that governs *Drosophila* male courtship behavior. *Cell.* 2005;121(5):795-807. PubMed PMID: 15935765.
56. Haussmann IU, White K, Soller M. Erect wing regulates synaptic growth in *Drosophila* by integration of multiple signaling pathways. *Genome Biol.* 2008;9(4):R73. Epub 2008/04/19. doi: gb-2008-9-4-r73 [pii]
10.1186/gb-2008-9-4-r73. PubMed PMID: 18419806; PubMed Central PMCID: PMC2643944.
57. Haussmann IU, Soller M. Differential activity of EWG transcription factor isoforms identifies a subset of differentially regulated genes important for synaptic growth regulation. *Dev Biol.* 2010;348:224-30.
58. Zaharieva E, Haussmann IU, Brauer U, Soller M. Concentration and localization of co-expressed ELAV/Hu proteins control specificity of mRNA processing. *Mol Cell Biol.* 2015;35(18):3104-15. Epub 2015/07/01. doi: MCB.00473-15 [pii]
10.1128/MCB.00473-15. PubMed PMID: 26124284.
59. Koushika SP, Soller M, DeSimone SM, Daub DM, White K. Differential and inefficient splicing of a broadly expressed *Drosophila* erect wing transcript results in tissue-specific enrichment of the vital EWG protein isoform. *Mol Cell Biol.* 1999;19(6):3998-4007.
60. Haussmann IU, Li M, Soller M. ELAV-mediated 3'-end processing of ewg transcripts is evolutionarily conserved despite sequence degeneration of the ELAV-binding site. *Genetics.* 2011;189(1):97-107. Epub 2011/06/28. doi: genetics.111.131383 [pii]

10.1534/genetics.111.131383. PubMed PMID: 21705751; PubMed Central PMCID: PMC3176107.

61. Livak KJ, Schmittgen TD. Analysis of relative gene expression data using real-time quantitative PCR and the 2(-Delta Delta C(T)) Method. *Methods*. 2001;25(4):402-8. Epub 2002/02/16. doi: 10.1006/meth.2001.1262

S1046-2023(01)91262-9 [pii]. PubMed PMID: 11846609.

62. Mackay TF, Richards S, Stone EA, Barbadilla A, Ayroles JF, Zhu D, et al. The *Drosophila melanogaster* Genetic Reference Panel. *Nature*. 2012;482(7384):173-8. Epub 2012/02/10. doi: 10.1038/nature10811. PubMed PMID: 22318601; PubMed Central PMCID: PMCPMC3683990.

63. Huang W, Massouras A, Inoue Y, Peiffer J, Ramia M, Tarone AM, et al. Natural variation in genome architecture among 205 *Drosophila melanogaster* Genetic Reference Panel lines. *Genome Res*. 2014;24(7):1193-208. Epub 2014/04/10. doi: 10.1101/gr.171546.113. PubMed PMID: 24714809; PubMed Central PMCID: PMCPMC4079974.

64. McDonald JH, Kreitman M. Adaptive protein evolution at the *Adh* locus in *Drosophila*. *Nature*. 1991;351(6328):652-4. Epub 1991/06/20. doi: 10.1038/351652a0. PubMed PMID: 1904993.

65. Tang H, Lewontin RC. Locating regions of differential variability in DNA and protein sequences. *Genetics*. 1999;153(1):485-95. Epub 1999/09/03. PubMed PMID: 10471728; PubMed Central PMCID: PMCPMC1460758.

66. Civetta A, Ostapchuk DC, Nwali B. Genome Hotspots for Nucleotide Substitutions and the Evolution of Influenza A (H1N1) Human Strains. *Genome Biol Evol*. 2016;8(4):986-93. Epub 2016/03/19. doi: 10.1093/gbe/evw061. PubMed PMID: 26988249; PubMed Central PMCID: PMCPMC4860693.

Figure legends

Figure 1: Mapping of sex-peptide insensitive EMS allele *QB62* to *Nup54*.

A) Schematic of the *Nup54* chromosomal region depicting gene models and chromosomal deficiencies used below the chromosomal nucleotide positions. Coding parts are shown as black and non-coding parts as white boxes. Transposon insert are show as triangles. The sequence of the deletion in *Nup54^{QB62}* and the promoter fragment used for genomic rescue construct *gNup54* are shown below the gene model.

B) Receptivity of wild type and transheterozygous *Nup54^{QB62}/Df(2R)9B4*, *Nup54^{MB03363}/Df(2R)9B4* and *Nup54^{MB03363}/Df(2R)9B4; gNup54* females after sex-peptide (SP, black) or Ringer's (R, white) injection measured by counting mating females in a 1 h time period 3 h after SP or R injection, respectively. Means with the standard error for three experiments with 18-23 females each are shown, and statistically significant differences are indicated by different letters ($p \leq 0.001$).

C) Oviposition of wild type and transheterozygous *Nup54^{QB62}/Df(2R)9B4*, *Nup54^{MB03363}/Df(2R)9B4* and *Nup54^{MB03363}/Df(2R)9B4; gNup54* females after sex-peptide (SP, black) or Ringer's (R, white) injection shown as means of eggs laid in 18 h with the standard error for 10 females each, respectively, and statistically significant differences are indicated by different letters ($p \leq 0.001$).

D) Number of stage 14 oocytes present in ovaries of sexually mature virgin wild type and transheterozygous *Nup54^{QB62}/Df(2R)9B4* and *Nup54^{MB03363}/Df(2R)9B4* females shown as means with the standard error for six ovaries.

E) Ribbon diagram of the structure of the channel Nup complex consisting of Nup54, Nup58 and Nup62 with the position of the *Mi{ETI}Nup54^{MB03363}* transposon indicated.

Figure 2: *Nup54* is required in *pickpocket* neurons to establish neuronal projections.

A-F) Larval ventral nerve cord expressing CD8::GFP from *UAS* by *ppkGAL4* in wild type (A-C) and *Nup54^{QB62}/Df(2R)9B4*. Magnified corresponding areas indicated in (D) are shown for wild type (B and C) and *Nup54^{QB62}/Df(2R)9B4* (E and F). Arrowheads indicate missing commissures or connectives.

G, H) Adult brain expressing CD8::GFP from *UAS* by *ppkGAL4* in wild type (G) and *Nup54^{QB62}/Df(2R)9B4* (H). Arrowheads point towards cell bodies of *ppk* expressing neurons with absent neuronal arborizations.

I) Adult brain expressing histon2B::YFP from *UAS* by *ppkGAL4* in wild type. Arrowheads point towards cell bodies of the four paired *ppk* expressing neurons in the adult brain. The scale bar in A is 50 μ m and in H is 100 μ m.

Figure 3: Brain *pickpocket* neurons are part of the circuit directing egg laying

A) Schematic of the intersectional gene expression approach to direct expression of mSP to brain *ppk* expressing neurons using brain expressed *otdflp* and *UAS FRTGFPstopFRTTNT*.

B) Receptivity of control and females expressing TNT in all (*ppkGAL4*) or only brain *ppk* neurons (*ppkGAL4 UAS stop TNT otdflp*) after sex-peptide (SP, black) or Ringer's (R, white) injection measured by counting mating females in a 1 h time period 3 h after SP or R injection, respectively. Means with the standard error for three experiments with 10-24 females each are shown, and statistically significant differences are indicated by different letters ($p \leq 0.05$).

C) Oviposition of control and females expressing TNT in all (*ppkGAL4*) or only brain *ppk* neurons (*ppkGAL4 UAS stop TNT otdflp*) after sex-peptide (SP, black) or Ringer's (R, white) injection shown as means of eggs laid in 18 h with the standard error for 12-30 females each, respectively. Statistically significant differences are indicated by different letters ($p \leq 0.001$).

D) Storage of stage 14 oocytes is not affected in virgin females expressing TNT in all (*ppkGAL4*) or only brain *ppk* neurons (*ppkGAL4 UAS stop TNT otdflp*). Means with the standard error from six ovaries each are shown, and statistically significant differences are indicated by different letters.

Figure 4: Nup54 promoter region is diverged in closely related species

A) Sequence alignment of the *Nup54* promoter region from closely related species. Nucleic acids deviating from *D. melanogaster* are indicated in black. Transcribed parts of the *DUBAI* 3'UTR and the *Nup54* 5'UTR, as well as the *Nup54^{QB62}* allele are underlined.

B) Plot of cumulative differences along the sequence (G) between the relative occurrences of nucleotide changes and their position from the alignment of the gene region around *Nup54* between *D. melanogaster* and *D. simulans*. Positions in the alignment with significant stretches of substitutions (hotspots) are identified by solid lines. The deletion in the *Nup54^{QB62}* allele indicated by a circle with a dashed line.

Figure 1 Haussmann et al

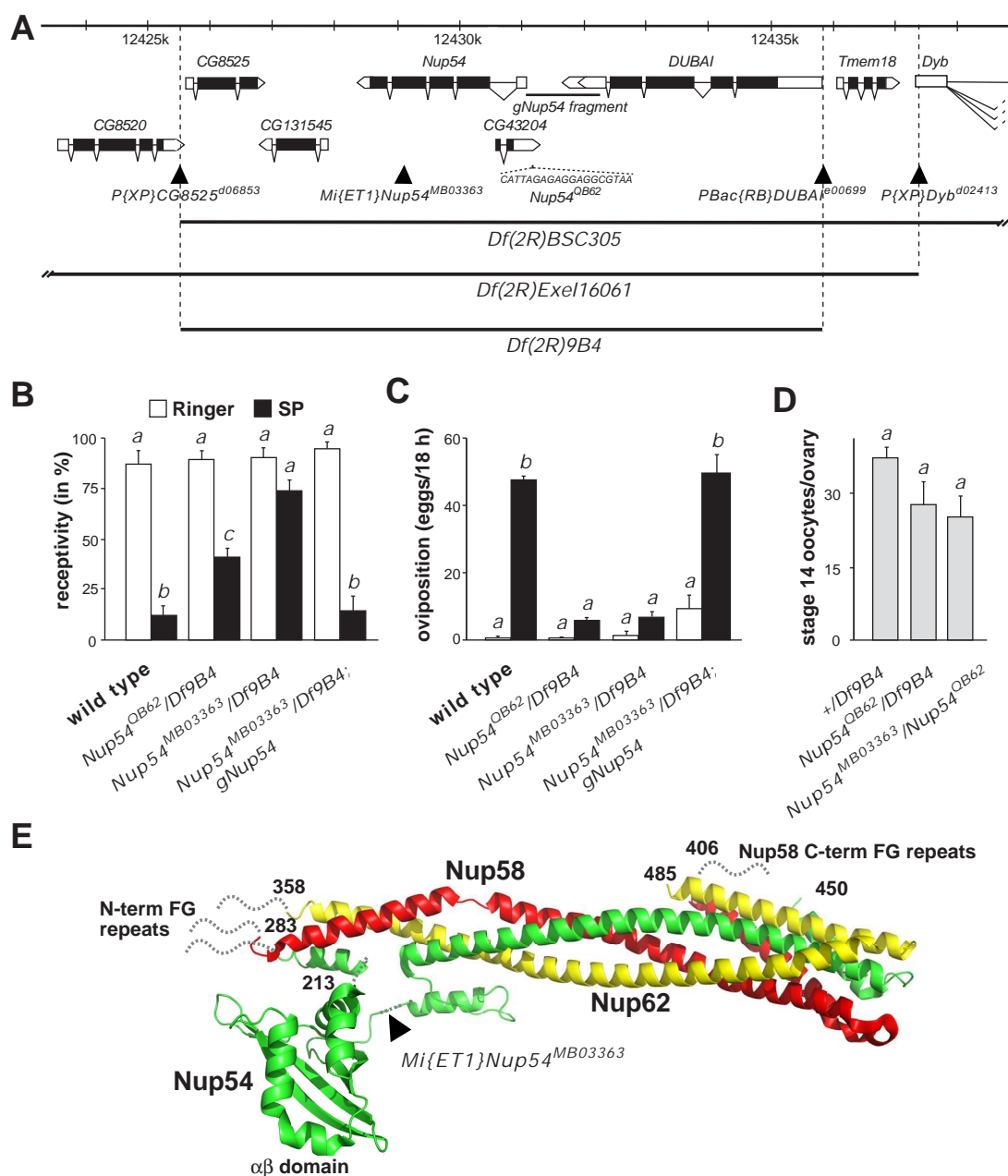


Figure 2
Haussmann et al

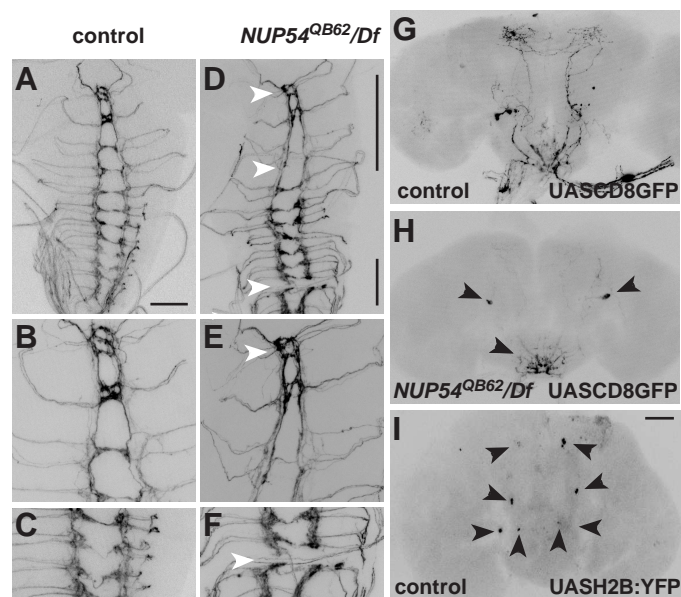


Figure 3
Haussmann et al

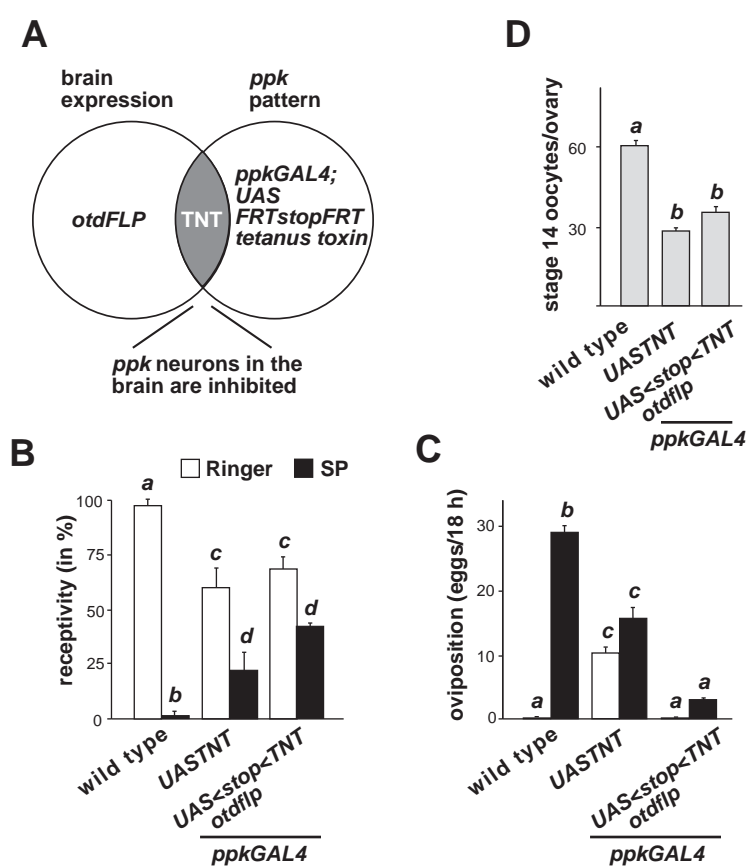
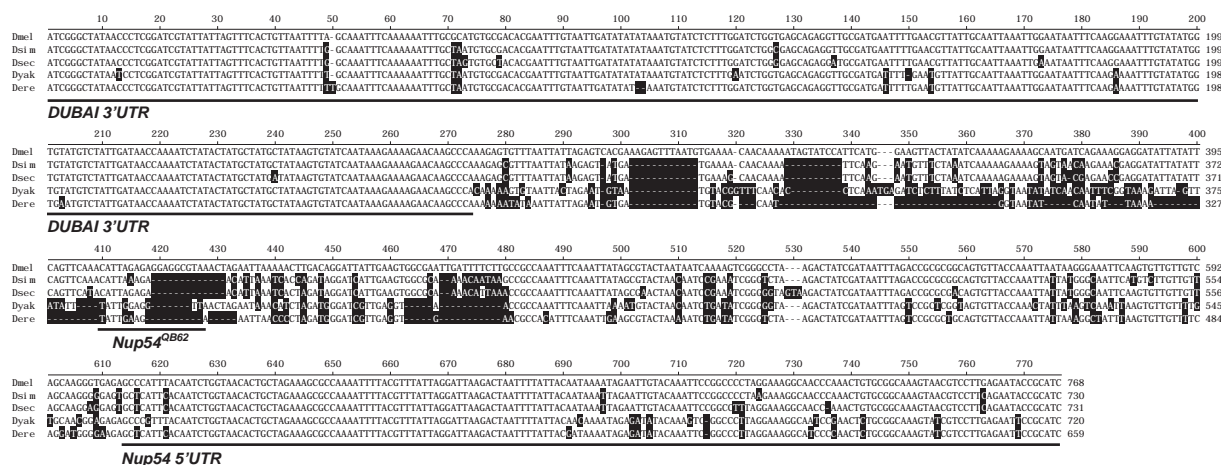
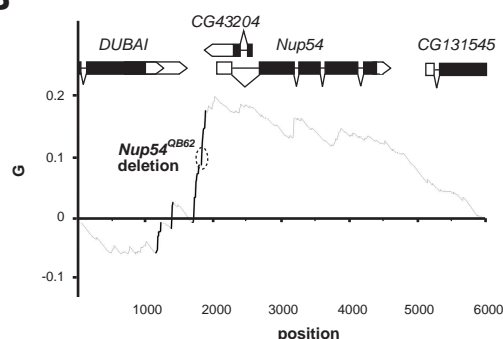


Figure 4 Haussmann et al

A



B



Supplementary Material for

Channel nuclear pore protein 54 prevents female *Drosophila* escape from male sex peptide

IRMGARD U. HAUSSMANN^{1,2*}, MOHANAKARTHIK P. NALLASIVAN^{1*}, DANIELA SCOCCHIA¹, ALBERTO CIVETTA³ AND MATTHIAS SOLLER^{1,4}

Supplementary Figures

Supplementary Figure S1: Nup54 is dynamically expressed in the brain.

A) RT-qPCR from RNA of adult female head and thorax of Nup54 in heterozygous *Nup54^{QB62}/+* and transheterozygous *Nup54^{QB62}/Df(2R)9B4* normalized to *erect wing* levels are shown as means from three replicates with standard error.

B) Expression of Nup54 expression from C-terminally HA tagged *gNup54* in *Df(2R)9B4* in salivary glands (i), the larval ventral nerve cord (ii) and the adult brain (iv) above nuclear DAPI staining and a merged picture with scale bars indicating 20 µm and 100 µm for salivary glands and brains, respectively. Higher magnification show variable Nup54 expression the larval ventral nerve cord (iii) and the adult brain (v) with scale bars indicating 10 µm.

Supplementary Figure S2: *Nup54* is required before neuronal maturation for establishing the post-mating response

A) Receptivity of control (blue) and transheterozygous *Nup54^{MB03363}/Df(2R)9B4* expressing *UASNup54::HA* with *tubGAL4* (purple) ubiquitously, in neurons with *elavGAL4^{C155}* (yellow) and in *ppkGAL4* (orange), *fruGAL4* (green) and *dsxGAL4* (red) patterns after sex-peptide (SP,

dark color) or Ringer's (R, light color) injection measured by counting mating females in a 1 h time period 3 h after SP or R injection, respectively. Means with the standard error for three experiments with 18-21 females each are shown, and statistically significant differences are indicated by different letters ($p \leq 0.001$).

B) Oviposition of control (blue) and transheterozygous *Nup54^{MB03363}/Df(2R)9B4* expressing *UASNup54::HA* with *tubGAL4* (purple) ubiquitously, in neurons with *elavGAL4^{C155}* (yellow) and in *ppkGAL4* (orange), *fruGAL4* (green) and *dsxGAL4* (red) patterns after sex-peptide (SP, dark color) or Ringer's (R, light color) injection shown as means of eggs laid in 18 h with the standard error for 10-16 females each, respectively, and statistically significant differences are indicated by different letters ($p \leq 0.001$).

Supplementary Figure S3: *Nup54 RNAi* in *doublesex* expressing neurons reveals a separable sex-peptide response in receptivity and oviposition and a role in sexual differentiation.

A) Receptivity after *Nup54 RNAi* knock-down from *UAS P{GD14041}v42153*; *P{GD14041}v42154* inserts in neurons with *elavGAL4^{C155}* (yellow) and in *ppkGAL4* (orange), *fruGAL4* (green) and *dsxGAL4* (red) patterns after sex-peptide (SP, dark color) or Ringer's (R, light color) injection measured by counting mating females in a 1 h time period 3 h after SP or R injection, respectively. Means with the standard error for three experiments with 16 females each are shown, and statistically significant differences are indicated by different letters ($p \leq 0.001$).

B) Oviposition after *Nup54 RNAi* knock-down from *UAS P{GD14041}v42153*; *P{GD14041}v42154* inserts in neurons with *elavGAL4^{C155}* (yellow) and in *ppkGAL4* (orange), *fruGAL4* (green) and *dsxGAL4* (red) patterns after sex-peptide (SP, dark color) or Ringer's (R, light color) injection shown as means of eggs laid in 18 h with the standard error for 8 females

($p \leq 0.001$).

C, D) Genitals of control females (C) and females expressing *Nup62 RNAi* from *UAS* with *dsxGAL4* (D). The scale bar in B is 20 μm .

E, F) Front legs of control males (E) and males expressing *Nup62 RNAi* from *UAS* with *dsxGAL4* (F). Arrowheads indicate the position sex combs. The scale bar in B is 100 μm .

Supplementary Figure S4: Expression of *Nup54*, *Nup58* and *Nup62*.

A-C) Profile of *Nup54*, *Nup58* and *Nup62* expression during development from RNA seq.

D-F) Profile of *Nup54*, *Nup58* and *Nup62* expression in various tissues from microarrays.

Supplementary Figure S5: *Nup54* is highly conserved, but variation in the FG repeat region is not the cause of an altered post-mating response.

A) Sequence alignment of *Nup54* from closely related species. Amino acids deviating from *D. melanogaster* are indicated in black. Intron positions are indicated by black arrowheads and the stop codon of the *Nup54^{MB03363}* allele is indicated by a red arrow head. Green and white filled arrowheads indicate maintained ($>1\%$) and rare ($<1\%$) polymorphisms with amino acid changes indicated on top. The line below the sequence indicates the NgoMIV-BamHI fragment that was replaced in the *gNup54elegans* construct. Nucleotides 1-115 according to human *Nup54* impasse the FG region, nucleotides 116-346 the α/β region and nucleotides 346-494 the α -helical region. The amino acids in exon 3 have been shown to bind to *Nup62* and the amino acids in exon 5 bind to *Nup58*.

B) Receptivity of wild type, *gNup54* and *gNup54elegans* females homozygous for *Df(2R)9B4* after sex-peptide (SP) or Ringer's (R) injection measured by counting mating females in a 1 hr time period 3 hr after SP or R injection, respectively. Means with the standard error for three

experiments with 8-15 females each are shown, and statistically significant differences are indicated by different letters.

C) Oviposition of *gNup54*, and *gNup54elegans* females homozygous for *Df(2R)9B4* after sex-peptide (SP) or Ringer's (R) injection shown as means of eggs laid in 18 h with the standard error for 10 females each, respectively. Statistically significant differences are indicated by different letters.

Figure S1
Haussmann et al

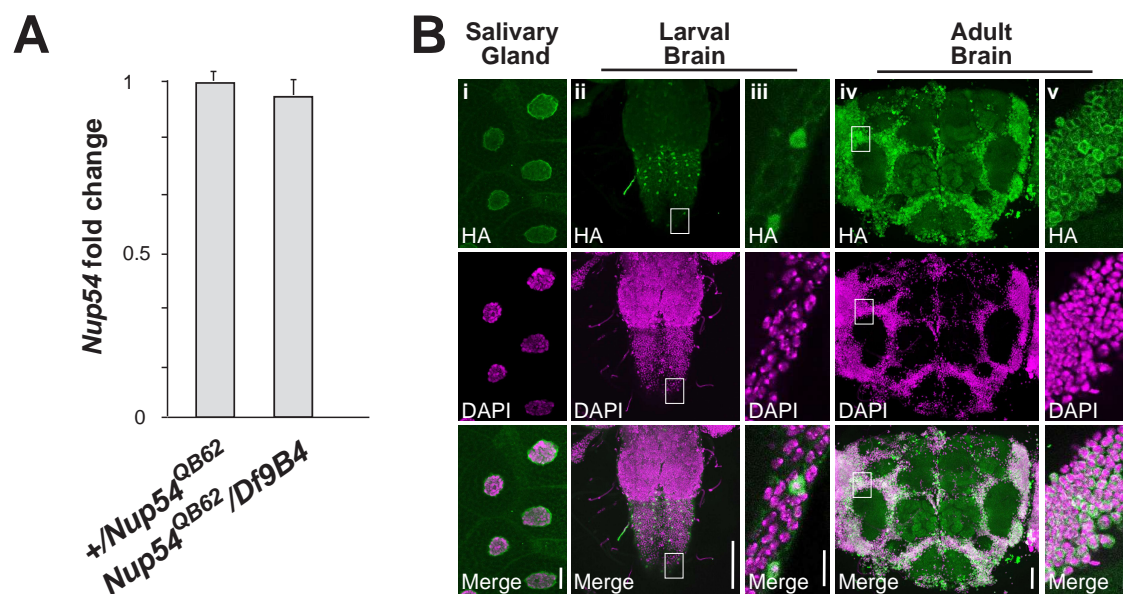


Figure S2
Haussmann et al

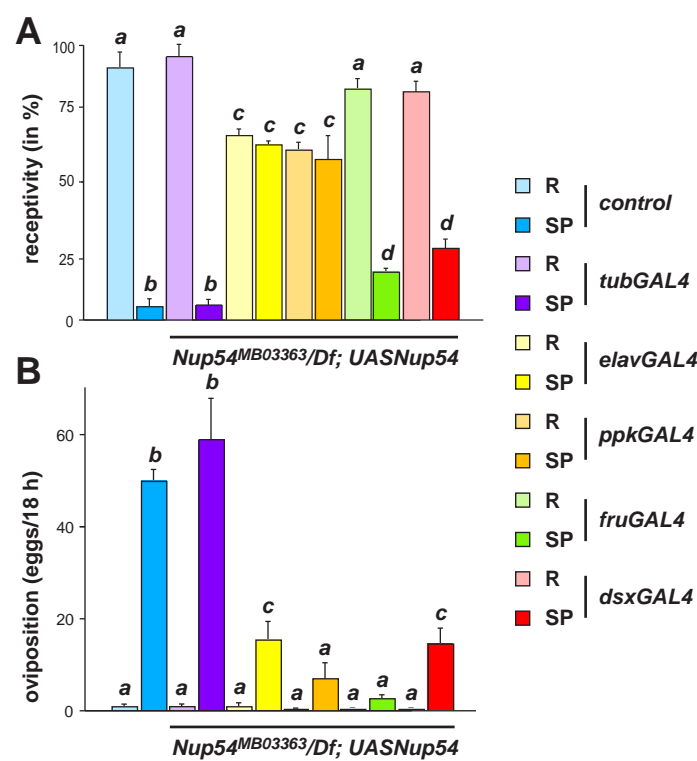


Figure S3
Haussmann et al

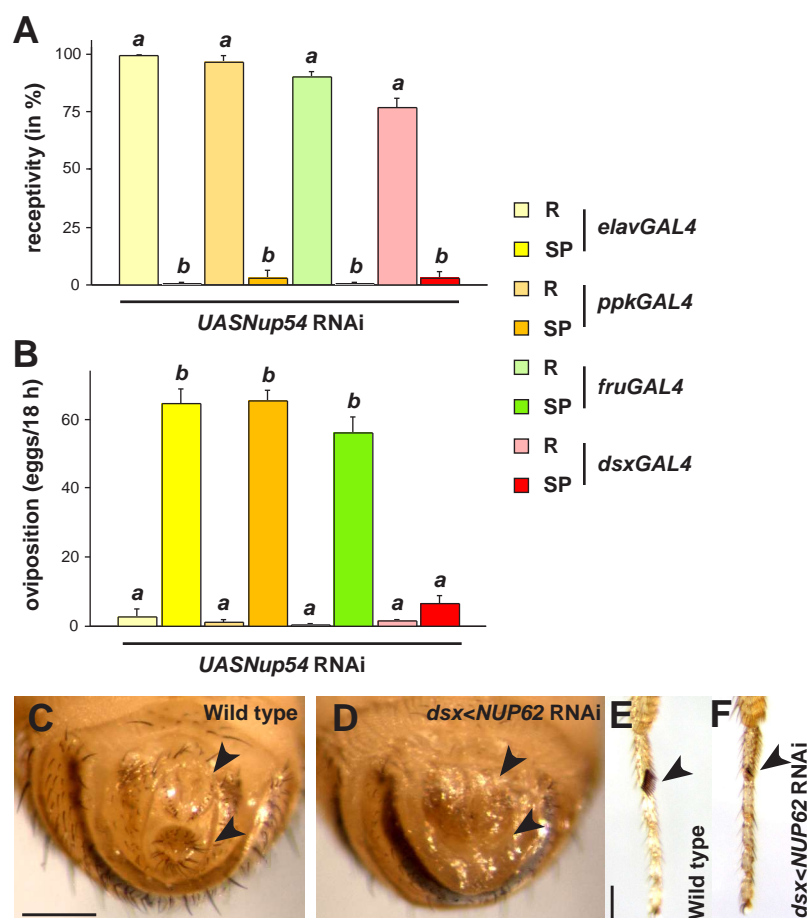


Figure S4
Haussmann et al

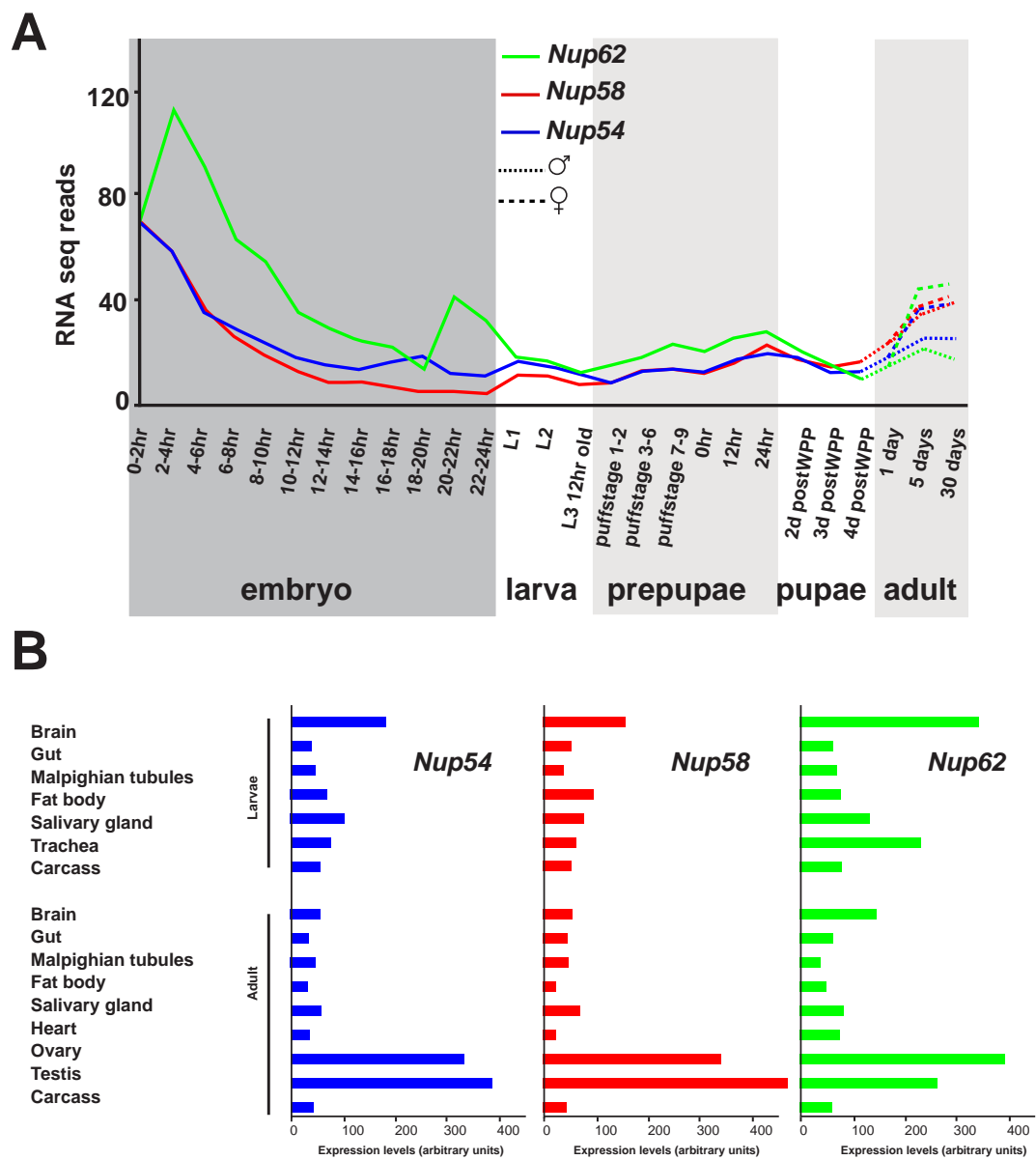


Figure S5 Haussmann et al

